# Supporting Information

## Janus building block-enabled fabrication of dual metal equipped coordination polymer: an ideal precursor for noble metal/metal oxide nanocomposites with excellent catalytic performance

Fang Cui, Qing Shao, Tieyu Cui,* Linxu Xu, Tongjie Yao and Xiao Zhang

The Academy of Fundamental and Interdisciplinary Science, Harbin Institute of Technology, Harbin 150001, PR China.

E-mail: cuit@hit.edu.cn; Fax: (+86) 451-86403646; Tel: (+86)451-86403646;

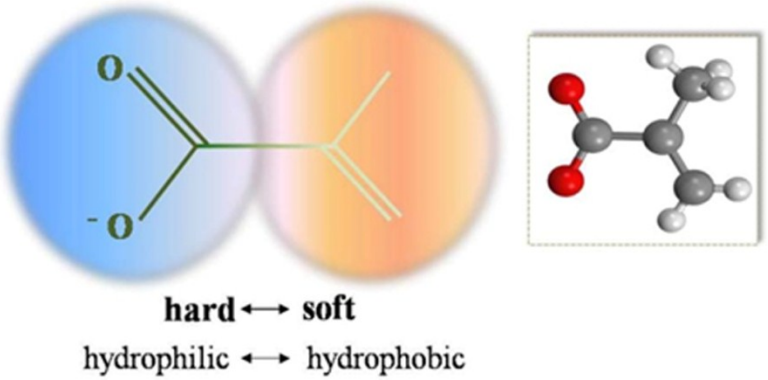


**Fig. S1** Molecular structure of the Janus MAA- ligand, which combines two parts with distinct characters.

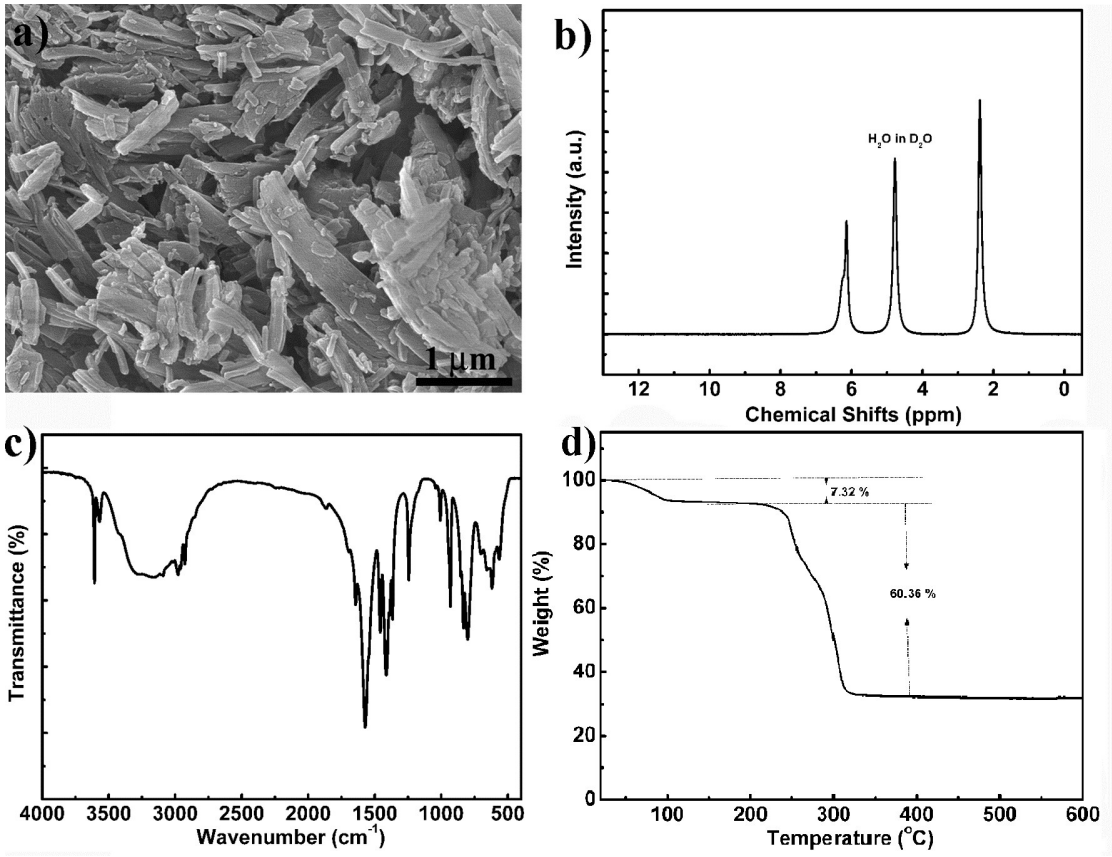


**Fig. S2** SEM image (a), $^{1}H$ NMR spectrum (b), FTIR spectrum (c) and TGA curve (d) of Co $(MAA)_2 \cdot H_2O$ precursors.

The $Co(MAA)_2 \cdot H_2O$ precursor exhibits irregular morphologies (Fig. S2(a)), and its chemical composition can be identified by $^{1}H$ NMR, FTIR, TGA and element analyses measurements. In the $^{1}H$ NMR spectrum (Fig. S2(b)), the chemical shifts around 2.38 and 6.14 ppm, with an integral ration of 3:2, are assigned to methyl and methylene protons of the methacrylate ion. FTIR spectrum (Fig. S2(c)) reveals the asymmetric (1567 $cm^{-1}$) and symmetric (1418 $cm^{-1}$) stretching vibrations of the carboxylate groups, indicating the coordination of $MAA^-$ to $Co^{2+}$. Elemental analysis on the as-made sample found [C (39.03%), H (4.81%)]. Co $(MAA)_2 \cdot H_2O$ is calculated to give [C (38.88 %), H (4.89 %)], matching closely the measured data. Furthermore, TGA data (obtained under $O_2$ atmosphere) is also consistent with the formula of Co $(MAA)_2 \cdot H_2O$. The weight loss of 7.32 % before 100 $^{o}C$ is assigned to the loss of crystal water (calc. 7.29 %). The weight loss of 60.36 % in the range of 195 to 320 $^{o}C$ corresponds to the loss of the organic components (calc. 60.23 %)

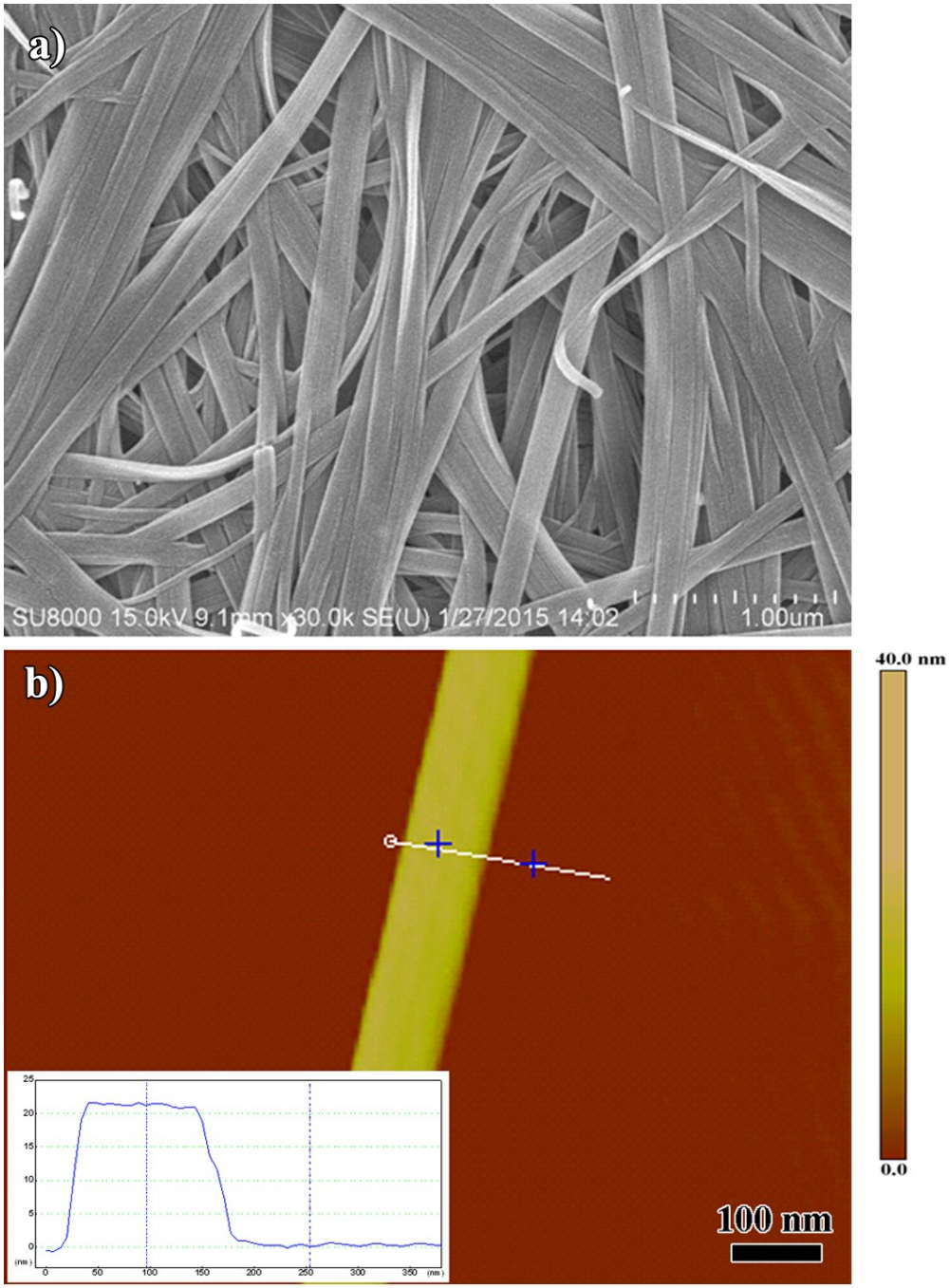


**Fig. S3** (a) SEM image of Co $(MAA)_2$ nanoribbons. (b) Tapping-mode AFM and corresponding topography cross section of the adherent $Co(MAA)_2$ nanoribbon on a silica wafer.

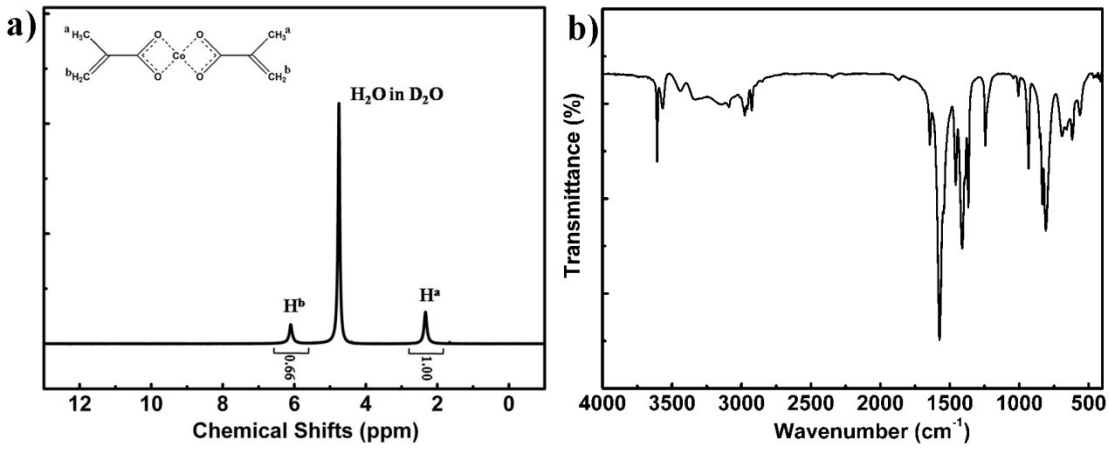


**Fig. S4** $^1$H NMR (a) and FTIR spectra (b) of Co $(MAA)_2$ nanoribbons.

The $^1$H NMR spectrum and detailed peak assignments of Co $(MAA)_2$ nanoribbons are shown in Fig. S4(a). The signals appearing at 2.33 and 6.10 ppm, with an integral ration close to 3:2, can be assigned to the methyl ($H^a$) and methylene ($H^b$) protons of the methacrylate ion ($MAA^-$). In the FTIR spectrum (Fig. S4(b)) of the Co $(MAA)_2$ nanoribbons, the presence of characteristic bands at around 1580 and 1410 cm $^{-1}$, belonging to the asymmetric and symmetric stretching vibrations of carboxylate groups respectively, indicates the successful coordination of methacrylate ion to cobalt ions. Moreover, element analysis was also used to identify the chemical composition of the nanoribbons. Elemental analysis on the as-made nanoribbons found [C (42.05%), H (4.31%)]. $Co(MAA)_2$ is calculated to give [C (41.94 %), H (4.40 %)], matching closely the measured data. All these characterizations confirm that the $MMA^-$ is the only ligand bonding the metal centers, and the molecule formula of the nanoribbons is $Co(MAA)_2$.

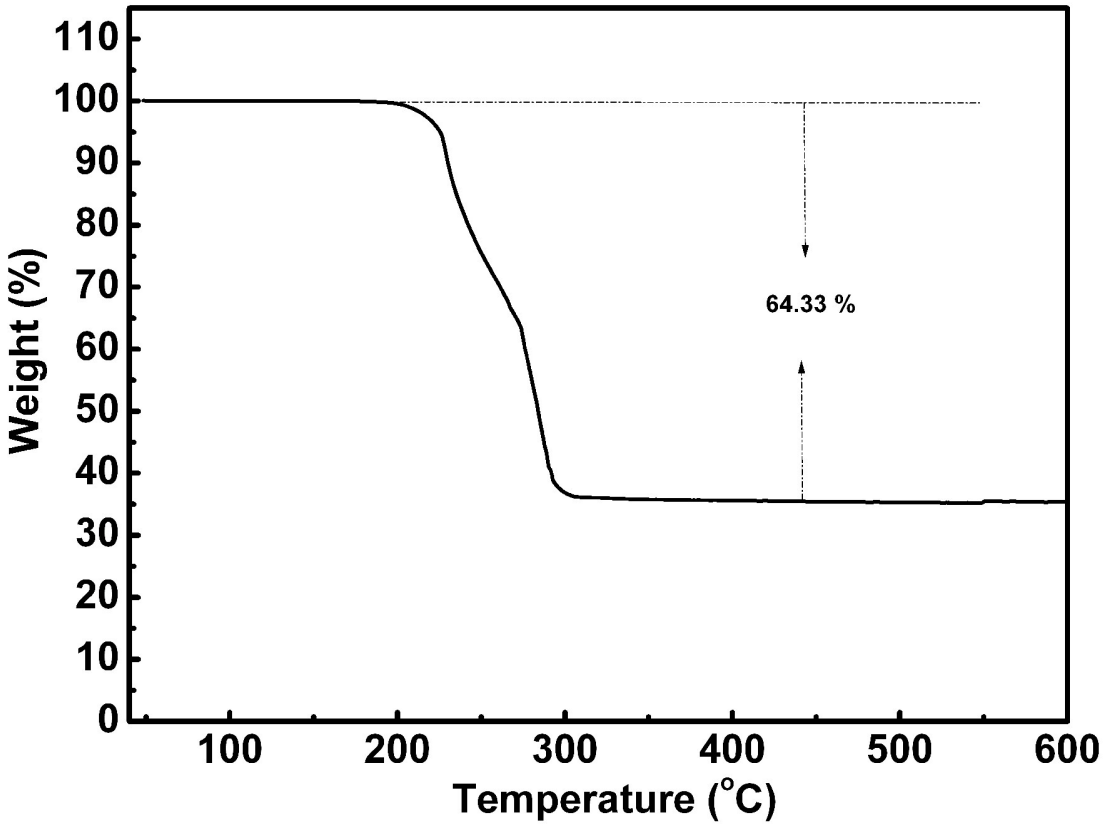


**Fig. S5** TGA curve of $Co(MAA)_2$ nanoribbons measured under oxygen atmosphere (heating rate: 10 $^oC$/min).

From the TGA curve of the $Co(MAA)_2$ nanoribbons, we can seen the nanoribbons start to decompose under $O_2$ atmosphere at around 195 $^oC$. The complete decomposition temperature is about 306 $^oC$. TGA data further confirms the molecule formula of the as-prepared Co $(MAA)_2$ nanoribbons. The weight loss in the range of 195 to 320 $^oC$ corresponding to the loss of the organic bridging ligands is about 64.33 %, which is in agreement with the calculated value of 64.96 %.

**Table S1.** XRD data for $Co(MAA)_2$ nanoribbons.

| $n_d$ | h k l | Calc. (2θ/°) | Obs. ( 2θ/°) | Difference (2θ/°) | Calc. (d/Å) | Obs. (d/Å) | Difference (d/Å) |
|---|---|---|---|---|---|---|---|
| 1 | 1 0 0 | 4.978 | 4.980 | 0.002 | 17.7376 | 17.7304 | -0.0072 |
| 2 | 1 0 1 | 6.260 | 6.250 | -0.010 | 14.1081 | 14.1301 | 0.0220 |
| 3 | 0 0 2 | 7.590 | 7.590 | 0.000 | 11.6381 | 11.6383 | 0.0002 |
| 4 | 0 1 1 | 8.832 | 8.830 | -0.002 | 10.0041 | 10.0064 | 0.0023 |
| 5 | 1 1 0 | 9.404 | 9.400 | -0.004 | 9.3971 | 9.4009 | 0.0038 |
| 6 | 1 1 1 | 10.143 | 10.150 | 0.007 | 8.7137 | 8.7079 | -0.0053 |
| 7 | 0 1 3 | 13.923 | 13.850 | -0.073 | 6.3554 | 6.3888 | 0.0334 |
| 8 | 3 0 0 | 14.971 | 14.970 | -0.001 | 5.9125 | 5.9133 | 0.0008 |
| 9 | 0 0 4 | 15.213 | 15.220 | 0.007 | 5.8191 | 5.8167 | -0.0024 |
| 10 | 1 0 4 | 16.016 | 16.000 | -0.016 | 5.5291 | 5.5348 | 0.0057 |
| 11 | 3 0 2 | 16.805 | 16.810 | 0.005 | 5.2713 | 5.2699 | -0.0014 |
| 12 | 3 1 0 | 16.984 | 16.970 | -0.014 | 5.2163 | 5.2206 | 0.0043 |
| 13 | 0 2 2 | 17.717 | 17.700 | -0.017 | 5.0021 | 5.0069 | 0.0048 |
| 14 | 3 1 2 | 18.625 | 18.610 | -0.015 | 4.7600 | 4.7641 | 0.0041 |
| 15 | 3 1 3 | 20.499 | 20.500 | 0.001 | 4.3289 | 4.3289 | 0.0000 |
| 16 | 4 1 2 | 22.894 | 22.900 | 0.006 | 3.8812 | 3.8804 | -0.0008 |
| 17 | 4 0 3 | 23.083 | 23.090 | 0.007 | 3.8500 | 3.8488 | -0.0010 |
| 18 | 0 3 1 | 24.382 | 24.380 | -0.002 | 3.6476 | 3.6480 | 0.0004 |
| 19 | 1 3 1 | 24.901 | 24.900 | -0.001 | 3.5728 | 3.5730 | 0.0002 |
| 20 | 5 0 2 | 26.241 | 26.240 | -0.001 | 3.3934 | 3.3935 | 0.0001 |
| 21 | 2 2 5 | 26.939 | 26.930 | -0.009 | 3.3070 | 3.3081 | 0.0011 |
| 22 | 4 0 6 | 30.593 | 30.590 | -0.003 | 2.9198 | 2.9201 | 0.0003 |
| 23 | 6 1 1 | 31.531 | 31.520 | -0.011 | 2.8351 | 2.8361 | 0.0010 |
| 24 | 0 4 0 | 32.292 | 32.290 | -0.002 | 2.7699 | 2.7701 | 0.0002 |

**Table S2.** The Kamlet-Taft parameters ($\alpha$: hydrogen-bond donor ability, β: hydrogen-bond acceptor ability) and dielectric constant (**ε**) of the solvents used in this study.

| Solvent | $\alpha$ | $\beta$ | $\varepsilon$ | Whether miscible with water? | Whether forming $Co(MAA)_2$ nanoribbon |
|---|---|---|---|---|---|
| **water** | 1.17 | 0.47 | 78 | Yes | No |
| **acetic acid** | 1.12 | 0.45 | 6 | Yes | No |
| **methanol** | 0.93 | 0.66 | 33 | Yes | No |
| **ethanol** | 0.83 | 0.75 | 25 | Yes | **Yes** |
| **isopropanol** | 0.76 | 0.84 | 20 | Yes | **Yes** |
| **dimethyl sulfoxide** (DMSO) | 0.00 | 0.76 | 47 | Yes | **Yes** |
| **dimethylformamide** (DMF) | 0.00 | 0.76 | 37 | Yes | **Yes** |
| **tetrahydrofuran** (THF) | 0.00 | 0.55 | 8 | Yes | **Yes** |
| **chloroform** | 0.20 | 0.10 | 5 | No | No |
| **n-hexane** | 0.00 | 0.00 | 2 | No | No |

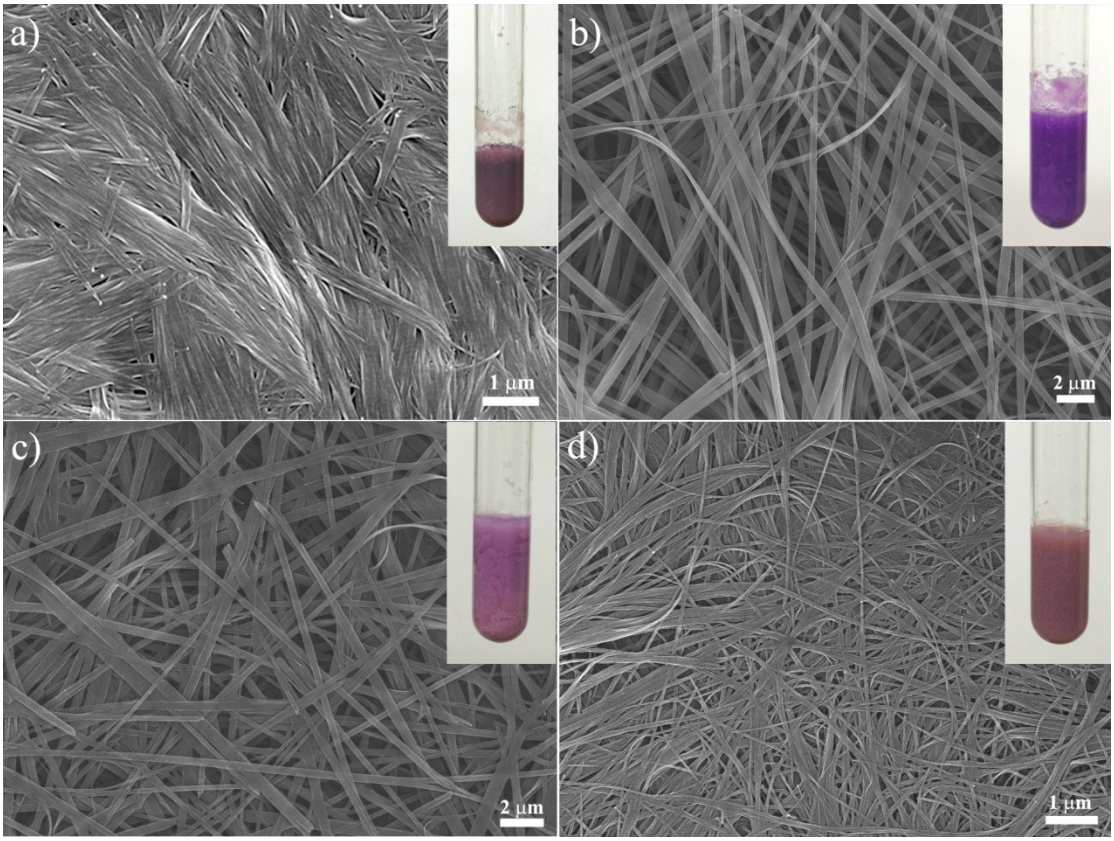


**Fig. S6** SEM images of the $Co(MAA)_2$ nanoribbons prepared by using isopropanol (a), DMSO (b), DMF (c) and THF (d) as the initiation solvents respectively. Insets: images showing the formation of a viscous gel upon generation of $Co(MAA)_2$ nanoribbons in corresponding initiation solvents.

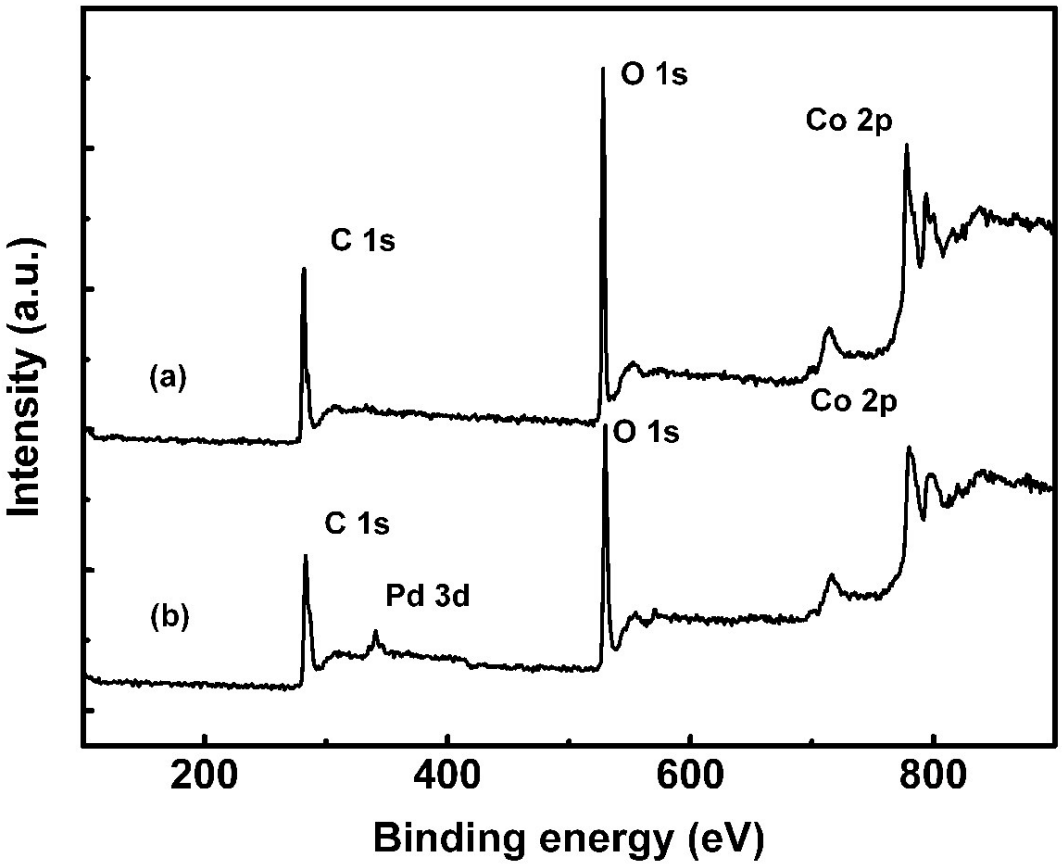


**Fig. S7** XPS spectra of Co $(MAA)_2$ (a) and $Co(MAA)_2$/Pd(II) nanoribbons (b).

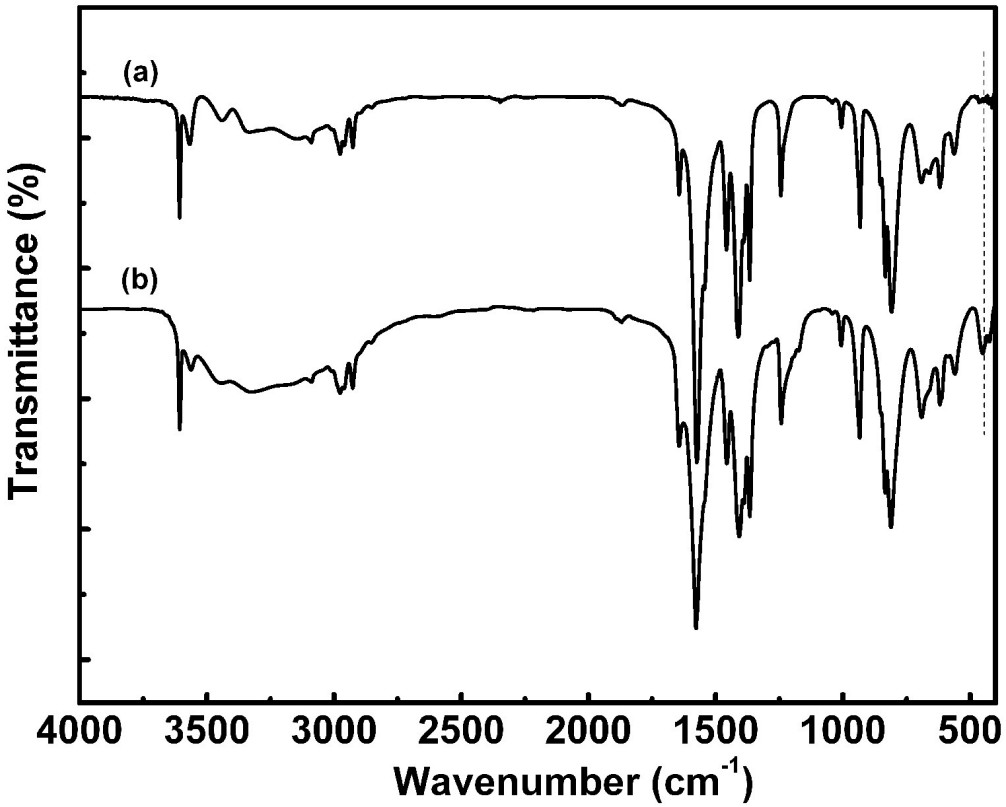


**Fig. S8** FTIR spectra of (a) $Co(MAA)_2$ and (b) $Co(MAA)_2$/Pd(II) nanoribbons. The peak around 430 $cm^{-1}$ corresponds to the Pd(II)-alkene stretching frequency, and is highlighted by the dotted line.

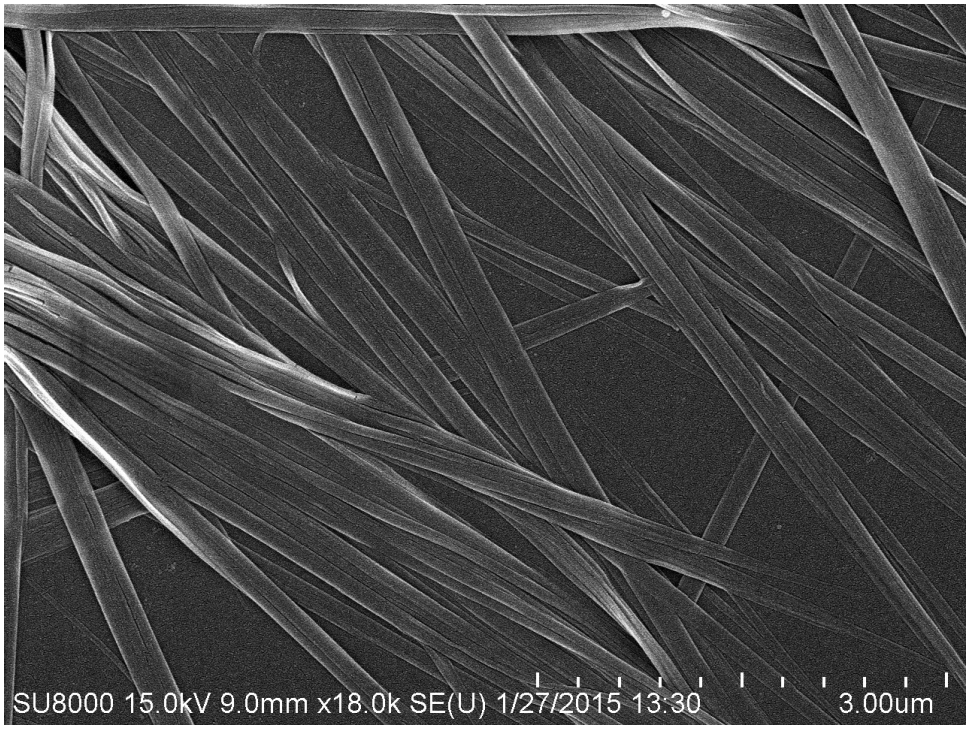


**Fig. S9** SEM image of the $Co(MAA)_2$/Pd(II) nanoribbons.

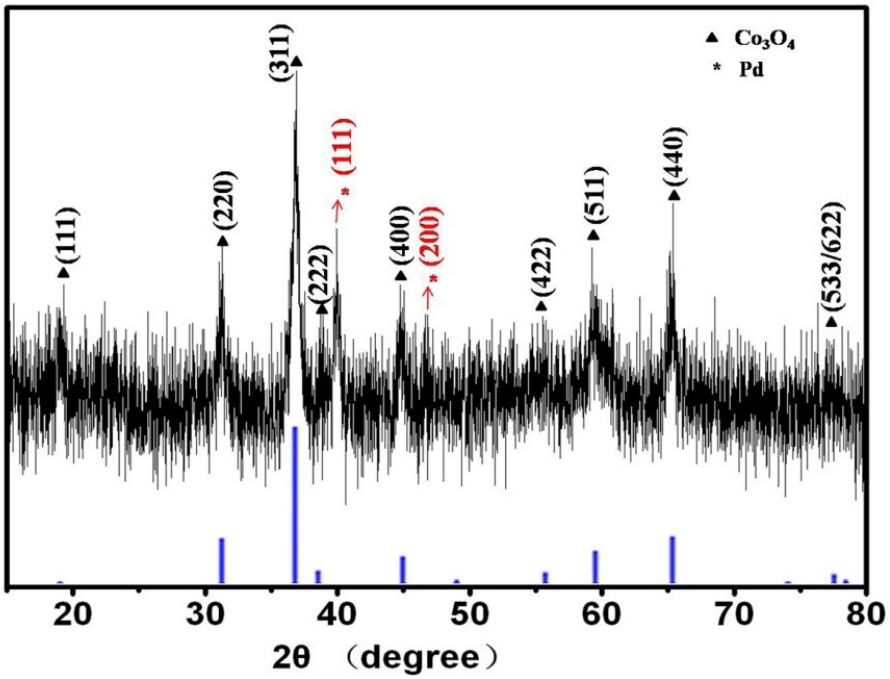


**Fig. S10** Powder XRD patter of $Pd/Co_3O_4$ composite nanoribbons.